

See discussions, stats, and author profiles for this publication at: <https://www.researchgate.net/publication/41893353>

Effects of Introducing Fibrinogen A α Character into the Factor XIII Activation Peptide Segment

ARTICLE *in* BIOCHEMISTRY · MARCH 2010

Impact Factor: 3.02 · DOI: 10.1021/bi902127u · Source: PubMed

CITATIONS

2

READS

15

4 AUTHORS, INCLUDING:



Toni A Trumbo

Bloomsburg University

9 PUBLICATIONS 154 CITATIONS

SEE PROFILE

Published in final edited form as:

Biochemistry. 2010 April 6; 49(13): 2918–2924. doi:10.1021/bi902127u.

Effects of Introducing Fibrinogen A α Character into the Factor XIII Activation Peptide Segment

Madhavi A. Jadhav[‡], Giulia Isetti[‡], Toni A. Trumbo[‡], and Muriel C. Maurer^{‡,*}

[‡]Department of Chemistry, University of Louisville, 2320 South Brook Street, Louisville, KY 40292

Abstract

The formation of a blood clot involves the interplay of thrombin, fibrinogen, and Factor XIII. Thrombin cleaves fibrinopeptides A and B from the N-termini of the fibrinogen A α and B β chains. Fibrin monomers are generated that then polymerize into a noncovalently associated network. By hydrolyzing the Factor XIII activation peptide segment at the R37-G38 peptide bond, thrombin assists in activating the transglutaminase FXIIIa that incorporates cross links into the fibrin clot. In the current research, the kinetic effects of introducing fibrinogen A α character into the FXIII AP segment were examined. About 25% of fibrinogen A α is phosphorylated at Ser 3 producing a segment with improved binding to thrombin. FXIII AP (²²AEDDL²⁶) has sequence properties in common with Fbg A α (¹ADSpGE⁵). Kinetic benefits to FXIII AP cleavage were explored by extending FXIII AP (28–41) to FXIII AP (22–41) and examining peptides with D24, D24S, D24Sp, and D24Sp P27G. These modifications did not provide the same kinetic advantages as observed with Fbg A α (1–20) S3p. Such results further emphasize that FXIII AP derives most of its substrate specificity from the P₉-P₁ segment. To enhance the kinetic properties of FXIII AP (28–41), substitutions were introduced at the P₉, P₄, and P₃ positions. Studies reveal that FXIII AP (28–41) V29F, V34G, V35G exhibits kinetic improvements that are comparable to FXIII AP V29F, V34L and approach those of Fbg A α (7–20). Selective changes to the FXIII AP segment sequence may be used to design FXIII species that can be activated more or less readily.

Thrombin, fibrinogen, and Factor XIII (FXIII)¹ play critical roles in the last stages of the blood coagulation cascade (1–4). Fibrinogen is a structural protein that circulates in the blood as a dimer of trimers (A α B β γ)₂. The serine protease thrombin cleaves the R16-G17 peptide bond of the fibrinogen A α chains and the R14-G15 peptide bond of the fibrinogen B β chains, thereby releasing fibrinopeptides A and B. These cleavages lead to exposure of fibrin polymerization sites that promote formation of a noncovalently associated fibrin clot network. Thrombin also supports Factor XIII activation by hydrolyzing the FXIII R37-G38 peptide bond which later aids in exposure of the transglutaminase catalytic site (3,4). Activated FXIII catalyzes the formation of γ -glutamyl- ϵ -lysyl covalent cross links in the fibrin network and in fibrin-enzyme complexes.

Thrombin is a versatile serine protease that targets several players in coagulation, anticoagulation, and platelet activation (1,5,6). This sodium activated type-II enzyme utilizes insertion loops on its surface to limit substrate access to the active site cleft. Moreover, thrombin contains two anion binding exosites (ABE-I and ABE-II) that it employs to promote interactions with selected proteins. See Figure 1. For example, regions of fibrinogen A α , PAR1,

* To whom correspondence should be addressed, Tel: 502-852-7008 Fax: 502-852-8149, muriel.maurer@louisville.edu.

¹Abbreviations: FXIII, blood clotting Factor XIII; AP, activation peptide; Fbg A α , fibrinogen A α chain; PAR1, protease activated receptor 1; PAR4, protease activated receptor 4; RP-HPLC, reversed phase high performance liquid chromatography; MALDI-TOF, matrix assisted laser desorption ionization time of flight; K_m, Michaelis-Menten kinetic constant; k_{cat}, catalytic constant or turnover number; NMR, nuclear magnetic resonance; NOESY, nuclear Overhauser effect spectroscopy; trNOESY, transferred NOESY.

hirudin, and thrombomodulin bind to ABE-I whereas fibrinogen γ' , heparin, GpIb α , and FVIII target ABE-II.

A review of thrombin substrates reveals that amino acids located N-terminal to the scissile bond make important contributions to binding and to rates of hydrolysis (7). The P₂, P₄, and P₉ positions² have been extensively studied. A common polymorphism exists in FXIII where a Val at the P₄ position is replaced with a Leu (V34L) (3). FXIII V34L is found in approximately 25% of the Caucasian population and results in a FXIII which is more easily activated by thrombin. This polymorphism has been correlated with protection against myocardial infarction (3,4). These effects occur predominantly under high fibrin(ogen) conditions and are associated with thinner fibrin chains and a more permeable clot structure (8).

Our laboratory has utilized kinetic studies and solution NMR methods to probe the roles of individual FXIII AP residues in interacting with thrombin. Trends observed with synthetic peptide models of the FXIII V34 and FXIII V34L activation segment are in agreement with results obtained with their intact FXIII species (9–13). A series of peptides with substitutions at the P₄ position (V, L, F, A, and I) have been screened for reactivity (14,15). The cardioprotective L34 continues to provide the strongest k_{cat}/K_m due to enhancements in K_m and even greater influences on k_{cat} . 2D trNOESY studies have revealed an important P₄ to P₂ interaction (L34/F34 to P36) that is proposed to promote interactions with the thrombin active site region (11,15).

In addition to the active site region, the anion binding exosites are also valuable to consider. A fibrinogen A α region located C-terminal to the thrombin-cleaved scissile bond targets ABE-I (2,5). By contrast, phosphorylation near the N-terminus allows this fibrinogen chain to be accommodated by thrombin ABE-II (16). The fibrinogen A α chain can be phosphorylated at two sites: the N-terminal S3 (17) and the more distant S345 (18). Increased levels of phosphorylation have been observed in certain physiological and pathophysiological conditions (19,20). Human fetal fibrinogen contains twice the degree of A α phosphorylation of adult fibrinogen (21). The amount of phosphorylated fibrinogen has been reported to double following hip replacement surgery (18). Elevated levels of phosphorylated fibrinogen have also been observed in cancer patients and in individuals recovering from acute myocardial infarction (22–25).

About 25–30% of plasma derived human fibrinogen A α (Fbg A α) is phosphorylated at the Ser3 position (26,27). Similar levels have been found in human fibrinogen chains expressed in CHO cells suggesting that partial phosphorylation is a native phenomenon (28). Kinetics studies on intact Fbg A α and on Fbg A α -like peptides (A α 1–20) have revealed that phosphorylation at the S3 position lowers the K_m of thrombin hydrolysis (16,29). Moreover, 1D and 2D NMR studies have shown that Ser3p helps to anchor A α 1–5 to the thrombin surface (16,30). A review of the Fbg A α residues ¹ADSp GE⁵ reveals that they have properties in common with FXIII AP (²²AEDDL²⁶). They both start with an alanine and then contain a series of negatively charged residues that could be accommodated by positively charged residues on an enzyme. These characteristics lead to an interest in exploring whether binding interactions between FXIII AP and the thrombin surface could be further enhanced by introducing a site of phosphorylation in which D24 is replaced with a phosphorylated serine (D24Sp). It is already known that residues within the FXIII P₉-P₁ segment make important contributions to binding and hydrolysis. The possibility of obtaining additional benefits from targeting ABE-II warrants further investigation.

²The P nomenclature system (...P₃, P₂, P₁, P₁', P₂', P₃'...) is used to assign the individual amino acid positions on the substrate peptides. The P₁-P₁' peptide bond becomes hydrolyzed by the enzyme. The peptide amino acids N-terminal to the cleavage site are labeled P₂, P₃, P₄ etc. whereas those that are C-terminal are labeled P₂', P₃', P₄' etc.

Another strategy to enhance the binding and hydrolysis of FXIII AP would be to introduce more Fbg A α -like character into the P₉-P₁ region. The Phe8 residue at the P₉ position of Fbg A α is vital for generating its effective thrombin substrate properties (31,32). A characteristic helical turn structure (33) is adopted in which the F8 is directed toward the P₄-P₁ region (¹³GGVR¹⁶). See Fig 2. V29F can be introduced into the FXIII AP sequence but there is concern how well the aromatic residue can be accommodated by the FXIII stretch ³⁴VVPR³⁷ (11). To alleviate possible steric issues, a FXIII AP peptide was proposed containing V29F, V34G, and V35G. The Pro at the P₂ position would remain since this residue plays a key anchoring role in the FXIII activation peptide sequence. The new sequence would thus contain substitutions at the P₉, P₄, and P₃ positions.

Our current work supports the proposal that FXIII derives most of its substrate specificity from P₉-P₁ with a focus on the P₄-P₁ segment. FXIII activation peptides that are extended to the P₁₆ position and further designed to target ABE-II do not exhibit the kinetic benefits observed for comparable fibrinogen A α -like sequences. Introducing other characteristic features of the A α chain into the FXIII AP segment is a more promising strategy to alter the activation properties of Factor XIII. For the mutant sequence FXIII AP (28–37) V29F, replacements of V34 and V35 with glycines promoted more effective binding and hydrolysis within the thrombin active site. Interestingly, the kinetic properties are comparable to those of FXIII AP (28–37) V29F, V34L. From these different studies, valuable information about the substrate specificity of thrombin for FXIII AP is being revealed.

Experimental Procedures

Synthetic Peptides

Peptides based on residues 22–41 of the human FXIII activation peptide were synthesized by New England Peptide (Gardner, MA) or by Giulia Isetti (University of Louisville), Louisville, KY. The peptide based on residues 28–41 was synthesized by SynPep (Dublin, CA). The peptide sequences are as follows: FXIII AP (22–41), Ac-AEDDLPTVELQGVVPRGVNL-amide; FXIII AP (22–41) D24S, Ac-AESDLPTVELQGVVPRGVNL-amide; FXIII AP (22–41) D24Sp, Ac-AESpDLPTVELQGVVPRGVNL-amide; FXIII AP (22–41) D24Sp P27G, Ac-AESpDLGTVELQGVVPRGVNL-amide; FXIII AP (28–41) V29F, V34G, V35G, Ac-TFELQGGGPRGVNL-amide. The purity of the peptides was evaluated by analytical reversed phase HPLC. MALDI-TOF mass spectrometry measurements on an Applied Biosystems Voyager DE-Pro mass spectrometer were used to verify the peptide *m/z* values. The concentrations of the peptide stock solutions were determined by quantitative amino acid analysis (AAA Service Laboratory, Damascus, OR and by University of Iowa, Molecular Analysis Facility, Iowa City, IA). All peptides were soluble to 8 mM.

Thrombin Preparation

Plasma bovine citrate or sulfate eluate (Sigma) was dissolved in 50mM Tris, 150mM NaCl, 0.1% PEG, pH 7.4 and desalted on an Amersham Pharmacia Biotech PD-10 column into the same buffer. The prothrombin containing solution was then activated at 37°C by *E. carinatus* snake venom in the presence of CaCl₂. The ability to clot fibrinogen was monitored over time. A Sephadex G-25 column equilibrated with 25mM H₃PO₄, 100mM NaCl, pH 6.5 was employed to desalt the venom-activated mixture. The generated thrombin was then purified on an Amersham Pharmacia Biotech Mono S cation exchange column (HR10/10) using a linear gradient of 0-1M NaCl in 25mM H₃PO₄, pH 6.5. The pooled thrombin solution was concentrated by ultrafiltration, aliquoted, and stored at –70°C. The final concentration of thrombin was determined using the extinction coefficient E^{1%} = 19.5 at 280 nm.

The bovine form of thrombin was used for this project and the synthetic substrates were based on human sequences. There is a high degree of sequence conservation between bovine and human thrombin (34). No differences appear in the residues involving the active site, the thrombin β -insertion loop (also called the Trp^{60D} loop), or the allosteric Na⁺ binding site. Any changes within ABE-II involve complementary substitutions between Lys and Arg residues. The other minor differences that do exist between the species are not anticipated to interfere with the interaction of the substrate peptides at the thrombin active site surface. Further supporting this notion, NMR studies (35–37) involving bovine thrombin and peptides targeting the active site (fibrinopeptide A and PAR1) have been in agreement with X-ray studies involving the same peptides in the presence of human thrombin (38,39). Furthermore, NMR studies involving γ' peptides that target ABE-II have revealed similar results for both bovine α -IIa and human γ -IIa (40).

Kinetics Procedure

The HPLC-based kinetic assay methods described in Trumbo and Maurer (9) was employed. Briefly, a solution of peptide and Assay Buffer (50 mM H₃PO₄, 100 mM NaCl, 0.1% PEG, pH 7.4) was heated to 25°C in a heat block. The peptide concentrations were within the range of 50 to 1500 μ M for the FXIII AP (22–41) peptide series [D24, D24S, D24Sp, and D24Sp P27G]. For FXIII AP (28–41) V29F, V34G, and V35G, the concentrations included 45–455 μ M. Hydrolysis was started by the addition of bovine thrombin. The thrombin concentration for the hydrolysis reactions was 33.6 nM for the FXIII AP (22–41) peptide series and 2.2 nM for the FXIII AP (28–41) V29F, V34G, and V35G. At regular intervals, an aliquot of the reaction mixture was removed and quenched in 12.5% H₃PO₄. A Brownlee Aquapore Octyl RP-300 C8 Cartridge column was used to separate the peptide peaks on a Waters HPLC system. Thrombin concentration and kinetic time points were chosen such that less than 15% of the total peptide concentration was hydrolyzed within 30 minutes. The FXIII AP (28–37) product peak was integrated and the peak area converted to concentration using a calibration curve.

The slopes of product concentration versus time plots were used to determine the initial velocities (in μ M/sec) for the different thrombin-catalyzed reactions. The results reported represent averages for at least three independent experiments. Kinetic values were calculated using non-linear regression analysis fit to the equation: $V = V_{\max} / (1 + K_m/[S])$ using the Marquardt-Levenberg algorithm in Sigma Plot (Jandel Scientific). K_m , V_{\max} , and k_{cat} were calculated from the coefficients of this equation. ANOVA calculations followed by Tukey-Kramer multiple comparisons were utilized for statistical analysis of the kinetics data (GraphPad, InStat Biostatistics, Version 3.0). The different kinetic constants determined for the current project were examined relative to values obtained from previous published studies that had all been carried out with bovine thrombin.

Results

Thrombin-Catalyzed Hydrolysis of FXIII Activation Peptides

An HPLC assay was used to monitor the hydrolysis rates of peptides based on FXIII AP (22–41) and on the peptide FXIII AP (28–41) V29F, V34G, V35G. For each peptide, thrombin cleaved at the R37-G38 amide bond and the substrates and hydrolyzed products eluted as distinct peaks on the Brownlee Aquapore C8 column. Hydrolyzed segments corresponding to FXIII AP (22–37) and FXIII AP (28–37) were verified by MALDI-TOF mass spectrometry. Accumulation of these individual products over time was used in the kinetic fit calculations.

Kinetic analysis of FXIII AP peptides that could extend from the thrombin active site towards anion binding exosite-II

Earlier studies in our laboratory reported the kinetic parameters associated with thrombin hydrolysis of FXIII AP (28–41) (9). In the current study, the FXIII AP segment length was increased N-terminally to FXIII AP (22–41). Table 1 displays this sequence along with others related to this project. Nonlinear regression analysis values for K_m , k_{cat} , and k_{cat}/K_m are shown in Table 2. The seven additional N-terminal residues present in FXIII AP (22–41) contributed to a 1.7-fold decrease in K_m relative to FXIII AP (28–41) ($P < 0.001$). This decrease corresponded to a moderate improvement in binding interactions.

A phosphorylated S3 at the P₁₄ position of Fbg A α (1–20) is known to promote binding of this peptide substrate to thrombin (16,29). FXIII AP (22–41) contains a D24 at the same position as the S3 of Fbg A α (1–20). A FXIII AP (22–41) D24S substitution was well tolerated and the kinetic binding properties remained statistically different from those of FXIII AP (28–41) ($P < 0.01$). Introducing a site of phosphorylation at S24 (D24Sp) resulted in some minor increases in K_m . Upon reviewing the FXIII AP (22–41) D24Sp sequence, there was concern that the P27 residue might promote a turn structure that hinders optimal interactions with thrombin ABE-II. To alleviate this possibility and introduce more flexibility, a glycine was introduced to produce FXIII AP (22–41) D24Sp, P27G. Only a very minor improvement in K_m occurred relative to FXIII AP (22–41) D24Sp. A review of the kinetic data revealed that there were no statistical differences in K_m values among the different variants of FXIII AP (22–41).

The k_{cat} values also provided valuable information about interactions between the FXIII AP segments and thrombin. The N-terminal extension to FXIII AP (28–41) to generate FXIII AP (22–41) resulted in a minor 1.3-fold decrease in k_{cat} ($P > 0.05$). This value was maintained with the D24S substitution. The k_{cat} value for FXIII AP (22–41) D24Sp increased to that of FXIII AP (28–41). The additional P27G mutation generated a FXIII AP (22–41) D24Sp, P27G peptide that exhibited about a two-fold decrease in k_{cat} value relative to FXIII AP (28–41). A convincing case for statistical differences in the k_{cat} values of the FXIII AP (28–41) and (22–41) peptide series could not be found.

Introducing Fibrinogen A α -like Character into FXIII AP (28–41)

Prior studies evaluated the effects of introducing V29F into FXIII AP (28–41) thus placing an aromatic residue (11) at the same position as the vital F8 of Fbg A α (7–20). See Tables 3 and 4. The K_m value for hydrolysis of FXIII AP (28–41) V29F improved 2.6-fold relative to wild type FXIII AP (28–41) ($P < 0.01$) whereas the k_{cat} value remained virtually unchanged. In the current studies, additional features of the Fbg A α chain were introduced. The newly modified FXIII AP segment contained the Phe residue (V29F) and the aliphatic branched V34, V35 residues were replaced with smaller G34, G35 residues (FXIII AP V29F, V34G, V35G: *TFELQGGGPRGVNL*, mutated residues in italics). The K_m of FXIII AP V29F, V34G, V35G ($326 \pm 79 \mu\text{M}$) was between that of FXIII AP (28–41) ($508 \pm 44 \mu\text{M}$) and FXIII AP (28–41) V29F ($195 \pm 34 \mu\text{M}$) ($P < 0.01$ for both comparisons). By contrast, the k_{cat} value of FXIII AP 22–41 (V29F, V34G, V35G) increased 4.5-fold relative to FXIII AP (28–41) and FXIII AP (28–41) V29F ($P < 0.001$). An evaluation of the resultant k_{cat}/K_m values revealed that the substrate specificity toward FXIII AP (V29F, V34G, V35G) was significantly different ($P < 0.001$) from FXIII activation peptides containing V34, V29F, or V34L. See Table 4. Interestingly, the K_m value of FXIII AP (V29F, V34G, V35G) was now comparable to that of Fbg A α (7–20). Furthermore, k_{cat} had improved such that it was now only 1.4-fold lower than that of Fbg A α (7–20).

Discussion

Factor XIII is activated in part when the serine protease thrombin cleaves the FXIII R37-G38 peptide bond (2–4). The current work provides an opportunity to evaluate the extent to which additional features from Fbg A α , a major physiological substrate, can be introduced into the FXIII AP sequence to promote binding interactions (K_m) and/or catalytic turnover (k_{cat}). The knowledge gained may be used in the design of new FXIII AP segments that can be activated to different extents.

Evaluating whether FXIII AP segments can be generated that take advantage of binding to anion binding exosite-II

A review of the FXIII AP sequence reveals that the N-terminal segment ($^{22}\text{AEDDL}^{26}$) has negative charge character resembling that of the N-terminal Fbg A α segment ($^1\text{ADSGE}^5$). The N-terminal Fbg A α 1–5 is quite flexible and designed to permit multiple conformations depending on the environment encountered. NMR and docking studies suggest that introducing a phosphoserine at position 3 (S3p) encourages contact with the thrombin surface. The phosphate is proposed to bind in the vicinity of R175 and R93 (16). See Figures 1 and 2. In response to the new substrate anchor point, a valuable improvement in K_m value occurs (16).

For the current study, the features of Fbg A α S3p were systematically introduced into the FXIII AP D24 position. Prior work had focused on FXIII AP (28–37) and on the truncated FXIII AP (33–37) sequence (9,41). Extending the FXIII AP segment toward A22 at the P_{16} position did provide some benefits to K_m , but the k_{cat} was negatively affected. A D24S substitution was well tolerated indicating that an acidic aspartate residue was not required for the P_{14} position of FXIII AP. Introducing the phosphorylated Ser (D24Sp) generated modest improvements in k_{cat} but the K_m also increased. Overall, the slight improvements in k_{cat}/K_m obtained with the N-terminal extension and the site of phosphorylation were not statistically significant (Table 2).

A recent X-ray crystal structure of a murine PAR4 segment ($^{51}\text{K-A}^{81}$) bound to murine thrombin (Figure 3A) revealed an important conformational feature to consider (42). G60 located at the P_1' position of this substrate sequence helps to initiate a turn followed by a short helical segment. Instead of extending from the thrombin active site to ABE-I, the PAR4 segment is redirected toward the thrombin autolysis loop located below the entrance to the active site. P62 plays a critical role in helping to achieve this structural change. See residue highlighted in yellow in Figure 3A. Interestingly, the FXIII AP segment contains a stretch with a Pro residue at the P_{11} position ($^{22}\text{AEDDLPTVEL}^{31}$). This ring structure may hinder the ability of the phosphorylated FXIII AP segment to target a complementary Arg or Lys residue within thrombin ABE-II (16). Extra flexibility was introduced through the double mutant D24Sp, P27G, but the new sequence did not provide extensive benefits. If anything, an ability to orient effectively within the thrombin active site region had become hindered.

The results obtained with this sequence design project lead to a reanalysis of the properties of FXIII and fibrinogen A α . When bound to thrombin, the fibrinogen A α segment ($^1\text{ADSGEGDFLAEGGGVR}^{16}$) adopts a unique helical-turn structure (33) with key participation from F8, L9, and $^{13}\text{GGVR}^{16}$ (Figure 2A). Such a structure has not been observed in solution NMR studies of FXIII AP V34, V34L, and V34F bound to thrombin (11,15). Fbg A α clearly requires an extension out to at least the P_9 residue and can gain further benefits by proceeding on to the P_{16} position and utilizing S3p at the P_{14} position. By contrast, kinetic studies with FXIII AP (22–41), FXIII AP (28–41), and the truncated segment FXIII AP (33–41) indicate that thrombin takes advantage of the P_9 – P_1 residues with a focus on the P_4 – P_1 region (41). Furthermore, results suggest that FXIII residues surrounding the P_4 position are

more important for controlling thrombin binding and hydrolysis than extending to a segment that could target ABE-II.

Evaluating the effects of introducing further Fbg A α -like character into FXIII AP (28–41)

The roles of the P₉ - P₁ positions in promoting thrombin catalyzed hydrolysis of FXIII AP segments are worth further exploring. The common polymorphism V34L results in a 2-fold improvement in K_m and more importantly a 3-fold improvement in k_{cat} relative to FXIII AP V34 (9). See Table 4. Overall, a 5-fold improvement in k_{cat}/K_m occurs with the addition of a methylene group to the V34 at the P₄ position. Introduction of V29F at the P₉ position (11) leads to a 2.6-fold improvement in K_m relative to FXIII AP (28–41) V34; however, there is no change to k_{cat}. Although the V29F substitution makes the FXIII AP segment more Fbg A α -like, the kinetic benefits found in the A α chain have not been achieved. Moreover, the characteristic helical turn structure of Fbg A α (7–16) is not observed in solution NMR studies of FXIII AP (28–37) V29F bound to thrombin (15).

To help promote optimal orientation of the FXIII V29F AP segment at the thrombin active site, the V34 and V35 residues at the P₄ and P₃ positions were replaced with glycines. Some decreases in binding interaction were observed, but more impressively, there was a 4.5-fold enhancement in catalytic turnover. To further improve k_{cat}, the next residue to mutate might be the P₂ position. Difficulties, however, will likely arise since FXIII AP (28–41) P36V exhibits solubility issues.

Unexpectedly, the kinetic properties of the FXIII AP (28–41) V29F, V34G, V35G peptide (²⁸TFELQGGGPRGVNL⁴¹) are very similar to those of FXIII AP (28–41) V29F, V34L (²⁸TFELQGLVPRGVNL⁴¹) (11). For each sequence, the P₉ and P₄-P₁ residues are underlined. Both peptides have comparable K_m values and they both exhibit the 4.5-fold improvement in k_{cat} over the FXIII AP (28–41) V34. In an earlier publication, the V34L at the P₄ position was proposed to play a more critical role than the V29F at the P₉ position (11). The V34L could influence K_m and k_{cat} whereas the V29F could only influence K_m. Solution NMR studies indicated that the hallmark P₄-P₂ interaction involving L34-P36 was preserved with FXIII AP V29F, V34L and a helical-turn involving F29 was still not visible (11). The current studies suggest that V34G, V35G substitutions at the P₄-P₃ positions can mimic the kinetic benefits of the V34L substitution at the P₄ position. The P₃ position exhibits much sequence variability and might not be expected to have a major contribution to substrate specificity. Work by Lee et al (43) revealed that recombinant FXIII A₂ V35L (at the P₃) does not exhibit the kinetic benefits of V34L. By contrast, Andersen and coworkers (44) reported that recombinant FXIII A₂ (V34L, V35T) results in a 7.6-fold increase in activation rate relative to FXIII A₂ V34 and a 5-fold increase relative to FXIII A₂ V34L. The current research indicates another P₄-P₃ double substitution (V34G, V35G) that can exhibit beneficial effects toward thrombin-catalyzed hydrolysis of the FXIII AP segment. The improvements with FXIII AP (V29F, V34G, V35G) are comparable to those of (V29F, V34L).

Determining the structural features of thrombin-bound FXIII AP (28–37) V29F, V34G, V35G and comparing them to the previously published FXIII AP sequences would be valuable. Unfortunately, it has not been possible to examine the triply substituted peptide using 1D proton line broadening and 2D trNOESY. The peptide does not exhibit fast enough exchange on/off the enzyme surface. This slow exchange does, however, support the proposal that the substitutions at the P₉, P₄, and P₃ positions have generated a peptide that exhibits increased affinity for the thrombin surface.

The ability to create a FXIII AP (28–41) segment that mimics the properties of Fbg A α (7–20) leads to the question of whether a true hybrid FXIII AP- Fbg A α sequence could be effective. Andersen and coworkers recently published their results on such a system (44). Fbg A α (7–

15) and A α (7–20) were incorporated into recombinant FXIII A₂ in place of the FXIII AP (28–37 or 28–41) segment. Interestingly, these variants had thrombin activation rates that were 5% of the wild type FXIII A₂. Furthermore, they exhibited greatly reduced clot lysis times.

To be an effective thrombin substrate, the Fbg A α (7–20) segment must be able to adopt a turn conformation bringing the F8 into proximity of the R16-G17 cleavage site. This structural feature has been documented by both X-ray (33) and solution NMR methods (35,36). So far a helical turn conformation has not been observed in solution (11,15) with FXIII AP (28–37) V34, V34L, V34F, V29F, or the doubly substituted V29F, V34L. If such a conformation does exist, it must be fleeting in nature. An X-ray crystal structure of a thrombin-FXIII AP (28–37) V34 complex has captured this structural feature (45). See Figure 3B. This backbone conformation occurs even though the sequence identity of the P₁₀-P₁ residues of Fbg A α (7–16) and FXIII AP (28–37) is only 20% (46). By contrast, FXIII AP (28–37) V34L appears to adopt a more extended conformation within the crystal complex (45). Molecular docking studies (46) have further supported this type of structural feature for a V34L containing activation peptide.

The FXIII AP segment is 37 residues in length and X-ray crystallography on the intact protein suggests that each activation peptide straddles across the FXIII dimer interface (47). With the hybrid FXIII AP- Fbg A α sequence, it is highly likely that a helical turn must form for this segment to become an effective thrombin substrate. The low observed FXIII A₂ activation rates suggest there may be difficulties in achieving this conformational feature. The length of the FXIII AP segment may also be considered. The Fbg A α segment only contains six residues N-terminal to the Fbg A α 7–20 segment. The Fbg A α (1–5) stretch is proposed to be highly flexible but can be anchored to thrombin ABE-II through phosphorylation at S3p (16). The FXIII AP 1–27 segment is so much longer. It is not known how well a helical turn could be maintained with the 28–37 segment and to what extent the conformation and placement of the 1–27 segment would be affected.

The results with hybrid FXIII AP- Fbg A α demonstrate that the complete P₉-P₁ segment of Fbg A α can not be introduced successfully into intact FXIII A₂ (44). A strategy in which only a few residues are changed may be more effective in generating a FXIII with improved activation rates. In the current research, an effort has been made to keep the P36 as a P₂ anchor point and then make selective changes to the P₉, P₄, or P₄/P₃ positions. The peptides generated do not appear to have a requirement for a helical turn structure, yet, they can achieve kinetic parameters that approach those of Fbg A α (7–20). These sequences have the potential for being more successful candidates within FXIII A₂.

Conclusions

Kinetic studies on the roles of individual substrate positions are highly worthwhile for understanding the sources of thrombin specificity. Introducing a site of phosphorylation at the P₁₄ position of the thrombin substrate FXIII AP does not provide the benefits that are seen with a complementary Fbg A α sequence. Extra anchoring of FXIII toward the ABE-II region may not be needed. Moreover, additional competing interactions with thrombin ABE-II may not be physiologically attractive. For promoting initial fibrin formation, it may be more desirable to use the exosite to enhance fibrinopeptide A cleavage.

The present studies also further support the proposal that FXIII AP derives most of its substrate specificity from P₉-P₁ with a strong focus on the P₄-P₁ segment. The influential role of the P₄ position is well documented. The FXIII AP segment can be further optimized by adding other Fbg A α -like features. A V29F substitution introduces an aromatic residue that can promote binding interactions with the extended thrombin active site surface. Additional improvements can come with FXIII AP (V29F, V34G, and V35G). The fact that a V29F, V34L

substitution can also mimic such effects reinforces the critical role that the common polymorphism L34 plays in promoting the kinetic properties of the FXIII AP segment. So far, the vital helical turn conformation of Fbg A α (7–16) has not been observed in solution for FXIII AP segments bound to thrombin. Selective changes to the FXIII AP sequence that are not reliant on this distinct structural feature may provide greater versatility in designing new FXIII species. The current research has focused on amino acid substitutions to enhance K_m and/or k_{cat} whereas other residue changes would be needed to generate a FXIII that is more difficult to activate. The final architecture of a fibrin clot will be influenced by thrombin's interplay with components of fibrinogen (A α B β γ)₂ and the FXIII AP segment.

Acknowledgments

We appreciate helpful research discussions and critical evaluation of the manuscript from T.M. Sabo, R. Woofter, and P. Doiphode. We also thank R. Woofter for assistance in statistical analysis of the data.

Funding for this project is supported by NIH R01 HL68440

References

1. Di Cera E. Thrombin as procoagulant and anticoagulant. *J Thromb Haemost* 2007;5 Suppl 1:196–202. [PubMed: 17635727]
2. Weisel JW. Fibrinogen and fibrin. *Adv Protein Chem* 2005;70:247–299. [PubMed: 15837518]
3. Ariens RA, Lai TS, Weisel JW, Greenberg CS, Grant PJ. Role of factor XIII in fibrin clot formation and effects of genetic polymorphisms. *Blood* 2002;100:743–754. [PubMed: 12130481]
4. Muszbek L, Bagoly Z, Bereczky Z, Katona E. The involvement of blood coagulation factor XIII in fibrinolysis and thrombosis. *Cardiovasc Hematol Agents Med Chem* 2008;6:190–205. [PubMed: 18673233]
5. Lane DA, Philippou H, Huntington JA. Directing thrombin. *Blood* 2005;106:2605–2612. [PubMed: 15994286]
6. Di Cera E. Thrombin. *Mol Aspects Med* 2008;29:203–254. [PubMed: 18329094]
7. Backes BJ, Harris JL, Leonetti F, Craik CS, Ellman JA. Synthesis of positional-scanning libraries of fluorogenic peptide substrates to define the extended substrate specificity of plasmin and thrombin. *Nat Biotechnol* 2000;18:187–193. [PubMed: 10657126]
8. Lim BC, Ariens RA, Carter AM, Weisel JW, Grant PJ. Genetic regulation of fibrin structure and function: complex gene-environment interactions may modulate vascular risk. *Lancet* 2003;361:1424–1431. [PubMed: 12727396]
9. Trumbo TA, Maurer MC. Examining thrombin hydrolysis of the factor XIII activation peptide segment leads to a proposal for explaining the cardioprotective effects observed with the factor XIII V34L mutation. *J Biol Chem* 2000;275:20627–20631. [PubMed: 10801785]
10. Ariens RA, Philippou H, Nagaswami C, Weisel JW, Lane DA, Grant PJ. The factor XIII V34L polymorphism accelerates thrombin activation of factor XIII and affects cross-linked fibrin structure. *Blood* 2000;96:988–995. [PubMed: 10910914]
11. Trumbo TA, Maurer MC. Thrombin hydrolysis of V29F and V34L mutants of factor XIII (28–41) reveals roles of the P(9) and P(4) positions in factor XIII activation. *Biochemistry* 2002;41:2859–2868. [PubMed: 11851434]
12. Balogh I, Szoke G, Karpati L, Wartiovaara U, Katona E, Komaromi I, Haramura G, Pfliegler G, Mikkola H, Muszbek L. Val34Leu polymorphism of plasma factor XIII: biochemistry and epidemiology in familial thrombophilia. *Blood* 2000;96:2479–2486. [PubMed: 11001900]
13. Wartiovaara U, Mikkola H, Szoke G, Haramura G, Karpati L, Balogh I, Lassila R, Muszbek L, Palotie A. Effect of Val34Leu polymorphism on the activation of the coagulation factor XIII-A. *Thromb Haemost* 2000;84:595–600. [PubMed: 11057856]
14. Trumbo TA, Maurer MC. V34I and V34A substitutions within the factor XIII activation peptide segment (28–41) affect interactions with the thrombin active site. *Thromb Haemost* 2003;89:647–653. [PubMed: 12669118]

15. Isetti G, Maurer MC. Probing thrombin's ability to accommodate a V34F substitution within the factor XIII activation peptide segment (28–41). *J Pept Res* 2004;63:241–252. [PubMed: 15049836]
16. Maurer MC, Peng JL, An SS, Trosset JY, Henschen-Edman A, Scheraga HA. Structural examination of the influence of phosphorylation on the binding of fibrinopeptide A to bovine thrombin. *Biochemistry* 1998;37:5888–5902. [PubMed: 9558322]
17. Blombaeck B, Blombaeck M, Edman P, Hessel B. Amino-acid sequence and the occurrence of phosphorus in human fibrinopeptides. *Nature* 1962;193:833–834. [PubMed: 13870090]
18. Seydewitz HH, Kaiser C, Rothweiler H, Witt I. The location of a second in vivo phosphorylation site in the A alpha-chain of human fibrinogen. *Thromb Res* 1984;33:487–498. [PubMed: 6719396]
19. Martin SC, Ekman P, Forsberg PO, Ersmark H. Increased phosphate content of fibrinogen in vivo correlates with alteration in fibrinogen behaviour. *Thromb Res* 1992;68:467–473. [PubMed: 1341057]
20. Seydewitz HH, Witt I. Increased phosphorylation of human fibrinopeptide A under acute phase conditions. *Thromb Res* 1985;40:29–39. [PubMed: 4089825]
21. Witt I, Muller H. Phosphorus and hexose content of human foetal fibrinogen. *Biochim Biophys Acta* 1970;221:402–404. [PubMed: 5490244]
22. Gordon IO, Freedman RS. Defective antitumor function of monocyte-derived macrophages from epithelial ovarian cancer patients. *Clin Cancer Res* 2006;12:1515–1524. [PubMed: 16533776]
23. Wang X, Wang E, Kavanagh JJ, Freedman RS. Ovarian cancer, the coagulation pathway, and inflammation. *J Transl Med* 2005;3:25. [PubMed: 15969748]
24. Haglund AC, Ronquist G, Frithz G, Ek P. Alteration of the fibrinogen molecule and its phosphorylation state in myocardial infarction patients undergoing thrombolytic treatment. *Thromb Res* 2000;98:147–156. [PubMed: 10713316]
25. Ogata Y, Heppelmann CJ, Charlesworth MC, Madden BJ, Miller MN, Kalli KR, Cilby WA, Robert Bergen H 3rd, Saggese DA, Muddiman DC. Elevated levels of phosphorylated fibrinogen-alpha-isoforms and differential expression of other post-translationally modified proteins in the plasma of ovarian cancer patients. *J Proteome Res* 2006;5:3318–3325. [PubMed: 17137333]
26. Blomback B, Blomback M, Edman P, Hessel B. Human fibrinopeptides. Isolation, characterization and structure. *Biochim Biophys Acta* 1966;115:371–396. [PubMed: 5943441]
27. Blomback B, Blomback M, Searle J. On the occurrence of phosphorus in fibrinogen. *Biochim Biophys Acta* 1963;74:148–151. [PubMed: 13971745]
28. Binnie CG, Hettasch JM, Strickland E, Lord ST. Characterization of purified recombinant fibrinogen: partial phosphorylation of fibrinopeptide A. *Biochemistry* 1993;32:107–113. [PubMed: 8418831]
29. Hanna LS, Scheraga HA, Francis CW, Marder VJ. Comparison of structures of various human fibrinogens and a derivative thereof by a study of the kinetics of release of fibrinopeptides. *Biochemistry* 1984;23:4681–4687. [PubMed: 6238619]
30. Ni F, Konishi Y, Frazier RB, Scheraga HA, Lord ST. High-resolution NMR studies of fibrinogen-like peptides in solution: interaction of thrombin with residues 1–23 of the A alpha chain of human fibrinogen. *Biochemistry* 1989;28:3082–3094. [PubMed: 2742826]
31. Scheraga HA. Interaction of thrombin and fibrinogen and the polymerization of fibrin monomer. *Ann N Y Acad Sci* 1983;408:330–343. [PubMed: 6575693]
32. Scheraga HA. Chemical basis of thrombin interactions with fibrinogen. *Ann N Y Acad Sci* 1986;485:124–133. [PubMed: 3471143]
33. Martin PD, Robertson W, Turk D, Huber R, Bode W, Edwards BF. The structure of residues 7–16 of the A alpha-chain of human fibrinogen bound to bovine thrombin at 2.3-A resolution. *J Biol Chem* 1992;267:7911–7920. [PubMed: 1560020]
34. Bode W, Turk D, Karshikov A. The refined 1.9-A X-ray crystal structure of D-Phe-Pro-Arg chloromethylketone-inhibited human alpha-thrombin: structure analysis, overall structure, electrostatic properties, detailed active-site geometry, and structure-function relationships. *Protein Sci* 1992;1:426–471. [PubMed: 1304349]
35. Ni F, Meinwald YC, Vasquez M, Scheraga HA. High-resolution NMR studies of fibrinogen-like peptides in solution: structure of a thrombin-bound peptide corresponding to residues 7–16 of the A alpha chain of human fibrinogen. *Biochemistry* 1989;28:3094–3105. [PubMed: 2742827]

36. Ni F, Zhu Y, Scheraga HA. Thrombin-bound structures of designed analogs of human fibrinopeptide A determined by quantitative transferred NOE spectroscopy: a new structural basis for thrombin specificity. *J Mol Biol* 1995;252:656–671. [PubMed: 7563081]
37. Ni F, Ripoll DR, Martin PD, Edwards BF. Solution structure of a platelet receptor peptide bound to bovine alpha-thrombin. *Biochemistry* 1992;31:11551–11557. [PubMed: 1332764]
38. Mathews IL, Padmanabhan KP, Ganesh V, Tulinsky A, Ishii M, Chen J, Turck CW, Coughlin SR, Fenton JW 2nd. Crystallographic structures of thrombin complexed with thrombin receptor peptides: existence of expected and novel binding modes. *Biochemistry* 1994;33:3266–3279. [PubMed: 8136362]
39. Stubbs MT, Oschkinat H, Mayr I, Huber R, Anglikar H, Stone SR, Bode W. The interaction of thrombin with fibrinogen. A structural basis for its specificity. *Eur J Biochem* 1992;206:187–195. [PubMed: 1587268]
40. Sabo TM, Farrell DH, Maurer MC. Conformational analysis of gamma' peptide (410–427) interactions with thrombin anion binding exosite II. *Biochemistry* 2006;45:7434–7445. [PubMed: 16768439]
41. Isetti G, Maurer MC. Thrombin activity is unaltered by N-terminal truncation of factor XIII activation peptides. *Biochemistry* 2004;43:4150–4159. [PubMed: 15065858]
42. Bah A, Chen Z, Bush-Pelc LA, Mathews FS, Di Cera E. Crystal structures of murine thrombin in complex with the extracellular fragments of murine protease-activated receptors PAR3 and PAR4. *Proc Natl Acad Sci U S A* 2007;104:11603–11608. [PubMed: 17606903]
43. Lee IH, Chung SI, Lee SY. Effects of Val34Leu and Val35Leu polymorphism on the enzyme activity of the coagulation factor XIII-A. *Exp Mol Med* 2002;34:385–390. [PubMed: 12526104]
44. Andersen MD, Kjalke M, Bang S, Lautrup-Larsen I, Becker P, Andersen AS, Olsen OH, Stennicke HR. Coagulation factor XIII variants with altered thrombin activation rates. *Biological Chemistry*. 2009 in press.
45. Sadasivan C, Yee VC. Interaction of the factor XIII activation peptide with alpha -thrombin. Crystal structure of its enzyme-substrate analog complex. *J Biol Chem* 2000;275:36942–36948. [PubMed: 10956659]
46. Nair DG, Sunilkumar PN, Sadasivan C. Modeling of factor XIII activation peptide (28–41) V34L mutant bound to thrombin. *J Biomol Struct Dyn* 2008;26:387–394. [PubMed: 18808204]
47. Yee VC, Pedersen LC, Bishop PD, Stenkamp RE, Teller DC. Structural evidence that the activation peptide is not released upon thrombin cleavage of factor XIII. *Thromb Res* 1995;78:389–397. [PubMed: 7660355]

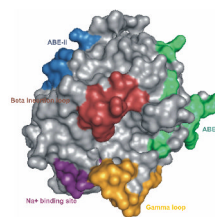


Figure 1. Structure of thrombin showing key surface loops and exosites

A contour representation of thrombin (PDB: 1PPB) is displayed with the active site region in the center. Beta and gamma loops that regulate substrate specificity and access to the catalytic site are shown respectively in maroon and yellow. Anion binding exosite I is located to the right of the active site region and is displayed in green whereas anion binding exosite II is located to the left and is displayed in blue. The allosteric sodium binding site is shown in purple. The molecular graphics program PyMOL was used to create the structures displayed in Figures 1–3.

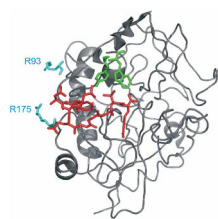


Figure 2. Evaluating thrombin interaction sites for the N-terminal Fbg Aα sequence

The X-ray crystal structure of human Fbg Aα (7–16) (red) bound to bovine thrombin (gray) is displayed (PDB: 1BBR). The thrombin β-insertion loop residues Trp60d and Tyr60a are highlighted in green. Two residues of anion binding exosite II (R93 and R175) that could accommodate Fbg Aα S3p are shown in light blue.

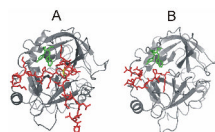


Figure 3. Comparing the conformational features of two thrombin:substrate complexes

A) A cartoon representation of murine PAR4 (51–81) (red) bound to murine thrombin (gray) is shown (PDB: 2PV9). Pro62 which is hypothesized to play a role in redirecting the PAR4 segment from the active site toward the thrombin autolysis loop is displayed in yellow. The thrombin β -insertion loop residues Trp60d and Tyr60a are highlighted in green. B) A cartoon representation of the X-ray crystal structure of FXIII AP (28–37) (red) bound to thrombin (gray) is displayed (PDB: 1DE7). The thrombin β -insertion loop residues Trp60d and Tyr60a are highlighted in green. So far the helical-turn conformation captured in the crystal structure has not been observed in solution by NMR methods.

Table 1Substrate Sequences Capable of Extending to Thrombin ABE-II^a

| | <i>P</i> ₉ <i>P</i> ₄ <i>P</i> ₁ ... |
|---|---|
| Factor XIII AP (22–41) | ²² AED DLPTVELQGVVPRGVNL ⁴¹ |
| Factor XIII AP (22–41) D24S | ²² AES DLPTVELQGVVPRGVNL ⁴¹ |
| Factor XIII AP (22–41) D24S _p | ²² AES _p DLPTVELQGVVPRGVNL ⁴¹ |
| Factor XIII AP (22–41) D24S _p P27G | ²² AES _p DLGTVELQGVVPRGVNL ⁴¹ |
| Fibrinogen Aα (1–20) S3 _p | ¹ ADS _p GEGDFLAEGGGVRGPRV ²⁰ |

^aHuman sequences of factor XIII and fibrinogen Aα are displayed. The Sp corresponds to a phosphorylated serine.

Table 2Kinetic constants for hydrolysis of FXIII AP substrates capable of extending to thrombin ABE-II ^a

| Peptide Sequence | K _m (μM) | k _{cat} (s ⁻¹) | k _{cat} /K _m (s ⁻¹ μM ⁻¹) |
|-------------------------------|---------------------|-------------------------------------|--|
| FXIII AP (28–41) ^b | 508 ± 44 | 6.4 ± 0.03 | 0.013 ± 0.001 |
| FXIII AP (22–41) | 300 ± 54 | 4.9 ± 0.01 | 0.016 ± 0.003 |
| FXIII AP (22–41) D24S | 270 ± 43 | 4.7 ± 0.31 | 0.017 ± 0.003 |
| FXIII AP (22–41) D24Sp | 422 ± 65 | 6.9 ± 0.48 | 0.016 ± 0.003 |
| FXIII AP (22–41) D24Sp, P27G | 370 ± 34 | 3.5 ± 0.15 | 0.009 ± 0.001 |

^a Kinetic constants for the thrombin-catalyzed hydrolysis reactions were determined from an HPLC assay as described in Materials and Methods. The results shown here represent averages of at least three independent experiments. Kinetic values were calculated using nonlinear regression analysis methods using SigmaPlot. The error values correspond to standard error of the mean (SEM).

^b Trumbo et al. (9)

Table 3Introducing Fibrinogen A α -like Character into the Factor XIII Activation Peptide^a

| | <i>P₉.....P₄...P₁...</i> |
|---|---|
| Factor XIII AP (28–41) | ²⁸ TVELQGVVPRGVNL ⁴¹ |
| Factor XIII AP (28–41) V34L | ²⁸ TVELQGLVPRGVNL ⁴¹ |
| Factor XIII AP (28–41) V29F | ²⁸ TFELQGVVPRGVNL ⁴¹ |
| Factor XIII AP (28–41) V29F V34L | ²⁸ TFELQGLVPRGVNL ⁴¹ |
| Factor XIII AP (28–41) V29F, V34G, V35G | ²⁸ TFELQGGGPRGVNL ⁴¹ |
| Fibrinogen A α (7–20) | ⁷ DFLAEGGGVRGPRV ²⁰ |

^aHuman sequences for factor XIII and fibrinogen A α are displayed.

Table 4Kinetic constants for hydrolysis of FXIII AP substrates having Fibrinogen A α -like character ^a

| Peptide Sequence | K _m (μ M) | k _{cat} (s ⁻¹) | k _{cat} /K _m (s ⁻¹ μ M ⁻¹) |
|--|---------------------------|-------------------------------------|---|
| FXIII AP (28–41) ^b | 508 \pm 44 | 6.4 \pm 0.03 | 0.013 \pm 0.001 |
| FXIII AP (28–41) V34L ^b | 272 \pm 57 | 18.5 \pm 1.6 | 0.068 \pm 0.02 |
| FXIII AP (28–41) V29F ^c | 195 \pm 34 | 6.2 \pm 0.4 | 0.032 \pm 0.006 |
| FXIII AP (28–41) V29F, V34L ^c | 352 \pm 77 | 27.5 \pm 2.9 | 0.078 \pm 0.02 |
| FXIII AP (28–41) V29F, V34G, V35G | 326 \pm 79 | 28.6 \pm 3.7 | 0.088 \pm 0.02 |
| Fbg A α (7–20) ^b | 312 \pm 42 | 39.3 \pm 2.6 | 0.126 \pm 0.02 |

^aKinetic constants for the thrombin-catalyzed hydrolysis reactions were determined from an HPLC assay as described in Materials and Methods. The results shown here represent averages of at least three independent experiments. Kinetic values were calculated using nonlinear regression analysis methods using SigmaPlot. The error values correspond to standard error of the mean (SEM).

^bTrumbo et al. (9)

^cTrumbo et al. (11)